**Immunity, Volume *56***

## Supplemental information

# Mural cell-derived chemokines provide a protective niche to safeguard vascular macrophages and limit chronic inflammation

**Kami Pekayvaz, Christoph Gold, Parandis Hoseinpour, Anouk Engel, Alejandro Martinez-Navarro, Luke Eivers, Raffaele Coletti, Markus Joppich, Flávio Dionísio, Rainer Kaiser, Lukas Tomas, Aleksandar Janjic, Maximilian Knott, Fitsumbirhan Mehari, Vivien Polewka, Megan Kirschner, Annegret Boda, Leo Nicolai, Heiko Schulz, Anna Titova, Badr Kilani, Michael Lorenz, Günter Fingerle-Rowson, Richard Bucala, Wolfgang Enard, Ralf Zimmer, Christian Weber, Peter Libby, Christian Schulz, Steffen Massberg, and Konstantin Stark**

Supplementary Figure 1

a

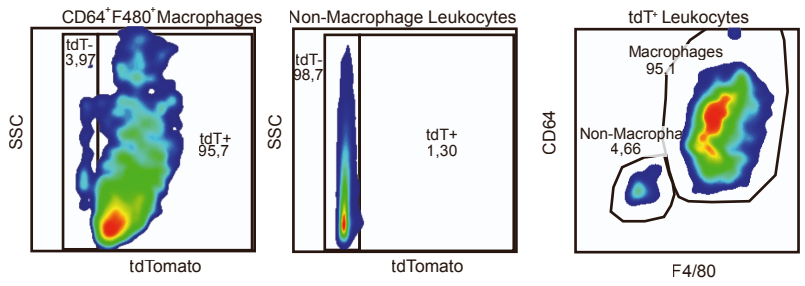


b

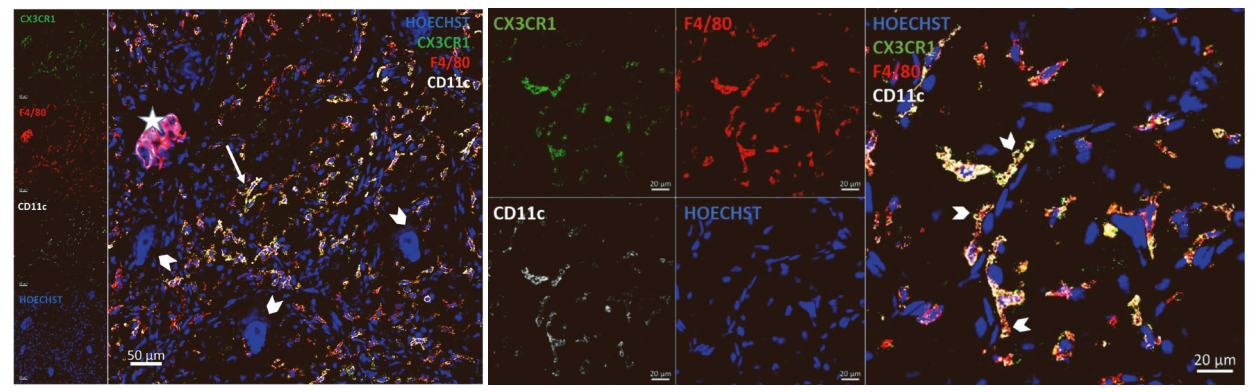


c

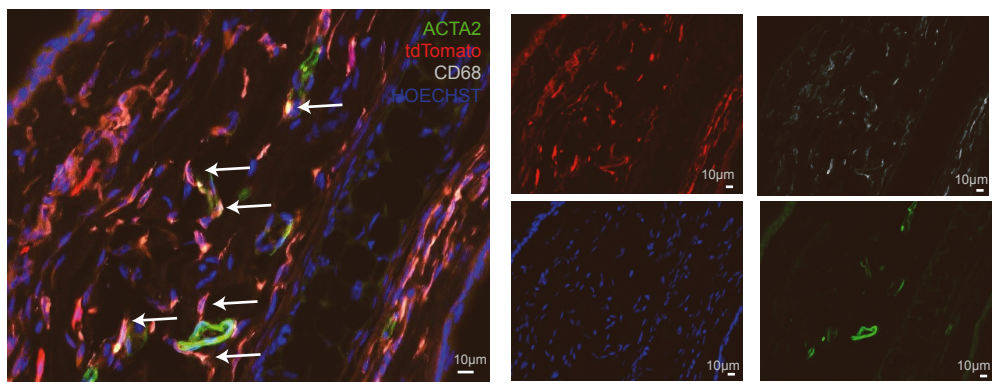


d

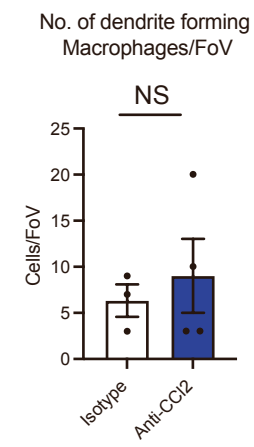


e

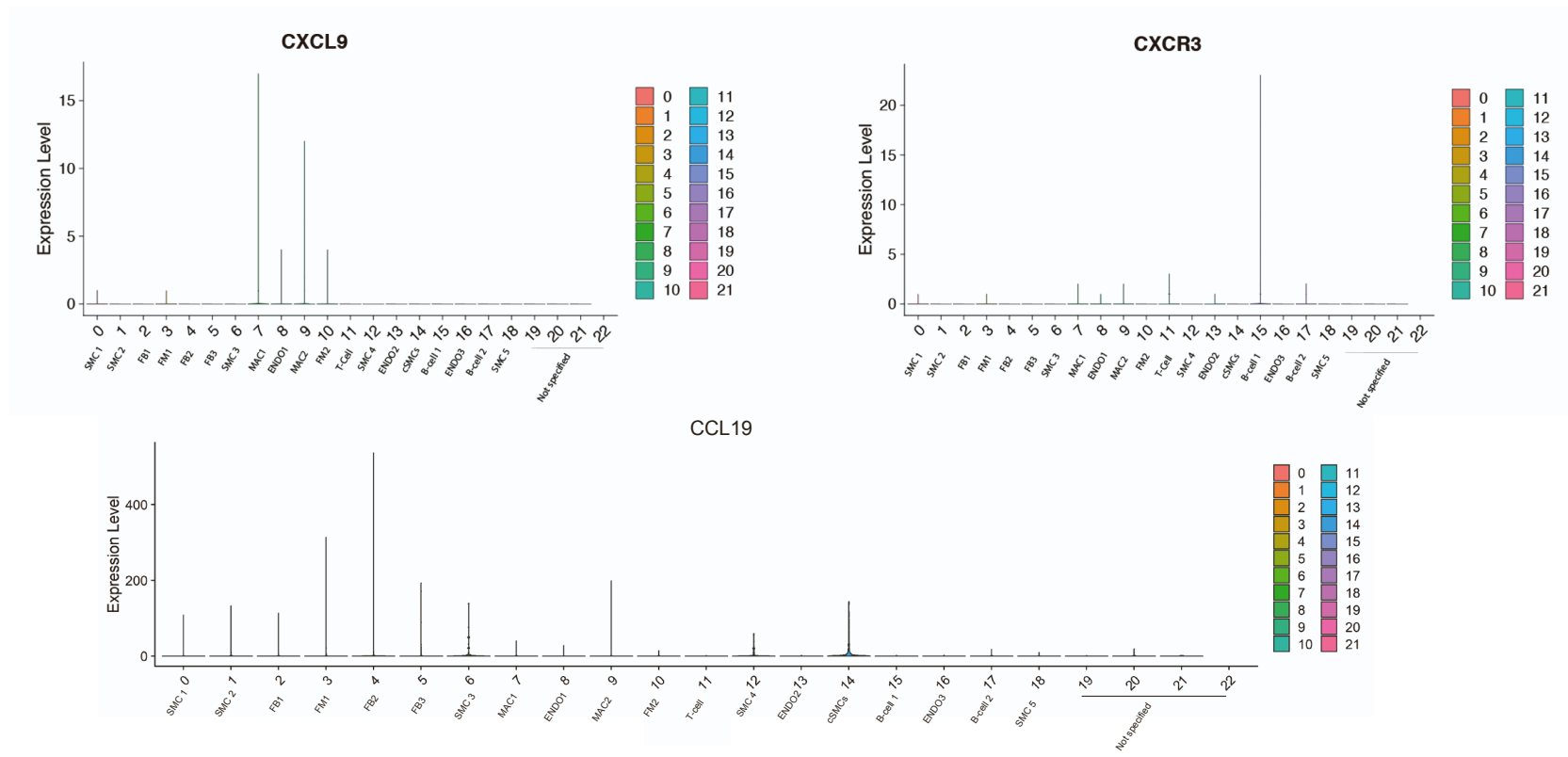


f

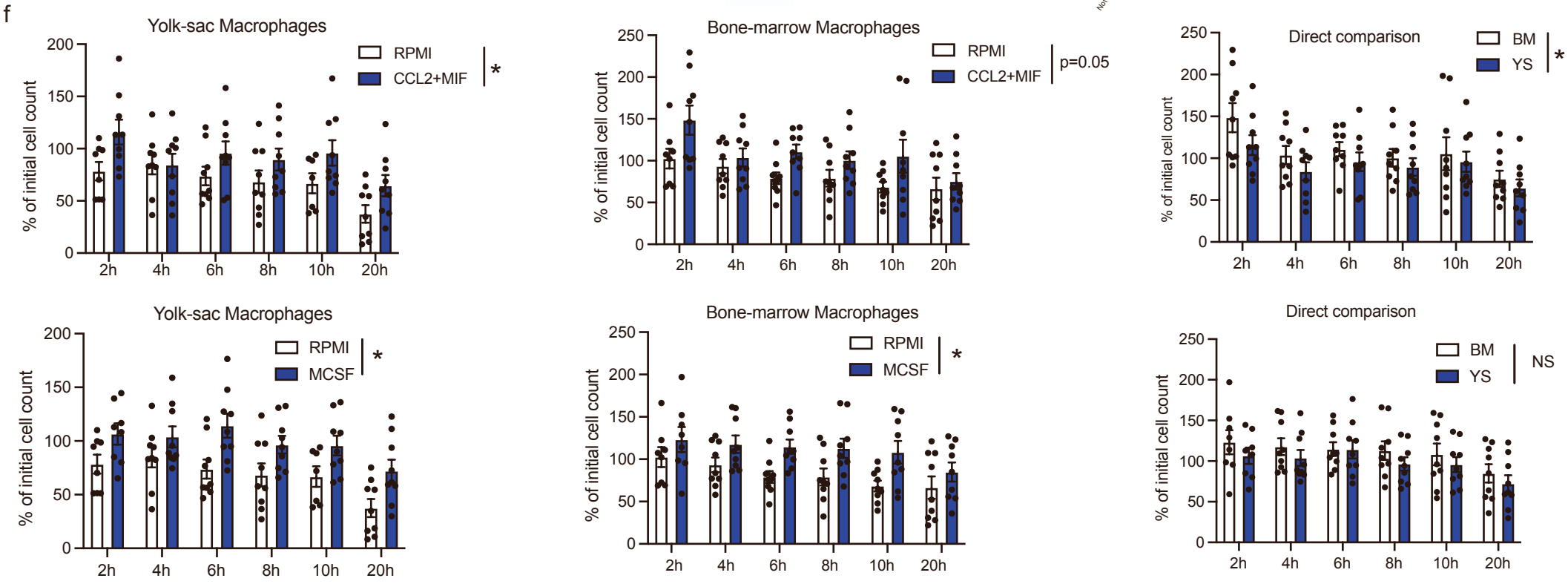


g

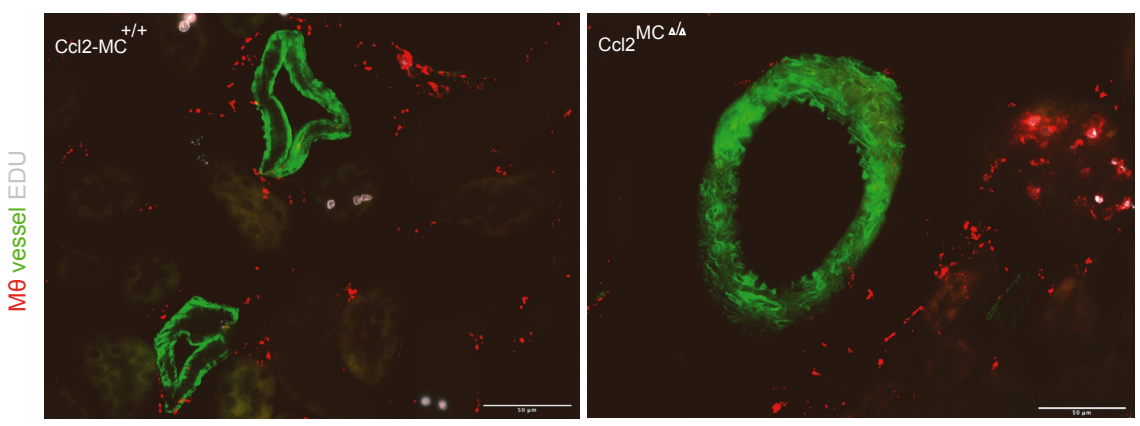


h

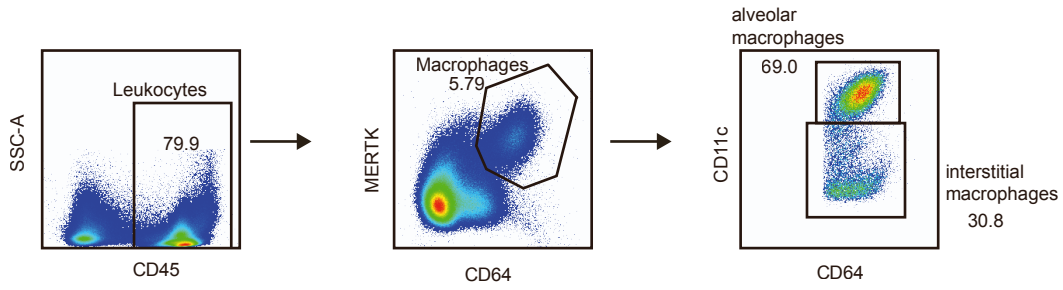


i

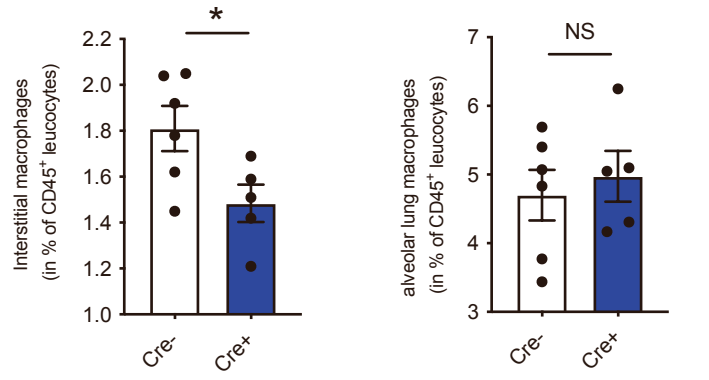

Suppl. Fig. 1 - Mural cells mediate MΦ survival (related to Figure 1): (**a**) Flow cytometry of Cx3cr1-MΦ$^{Ca\text{-}rep}$ mice, depicting a high proportion of tdTomato$^{+}$ cells among CD64$^{+}$ F4/80$^{+}$ MΦs (left), low number of tdTomato$^{+}$ cells among Non-MΦs (middle) and high proportion of MΦs among tdTomato$^{+}$ cells (right). Representative of 2 Cx3cr1-MΦ$^{Ca\text{-}rep}$ mice. (**b**) Dermal sheet whole mount *ex vivo* confocal imaging of skin tissue (ear) from a Cx3cr1-MΦ$^{GFP\text{-}rep}$ mice after *in vivo* laser injury, stained for F4/80 (red), HOECHST (blue), CD11c (white), endogenous Cx3cr1-GFP signal in green. Left image: Autofluorescent large laser injury is marked with white star. Small arrow-heads without a shaft mark hair follicles. Arrow with a shaft marks a MΦ forming a dendrite. Scalebar 50 µm. Right image: higher magnification of MΦs in skin tissue after sterile laser injury, small arrow-heads marking dendrites formed by MΦs. Scalebar 20 µm. (**c**) Confocal images of cross sections from skin (ear) of Cx3cr1-MΦ$^{Ca\text{-}rep}$ mice after staining for ACTA2 (green), CD68 (white), HOECHST (blue). Endogenous tdTomato in red. (**d**) Number of macrophages that extended at least one dendrite in the FOV during the imaging period in Cx3cr1-MΦ$^{GFP\text{-}rep}$ mice treated locally and systemically with isotype or CCL2-neutralizing antibody (averages from n=3-4 mice/group). (**e**) CXCL9, CXCR3, CCL19 expression levels across multiple clusters in human atherosclerotic lesions (Cluster definitions and UMAP in Fig. 3). (**f**) Quantification of MΦ survival in presence of CCL2 and MIF or M-CSF compared to control in yolk sac vs. bone marrow derived MΦs. n=9 replicates from 3 experiments. (**g**) Representative images from immunofluorescence staining of kidney sections in Ccl2$^{MC\Delta/\Delta}$ and Ccl2$^{MC+/+}$ mice for ACTA2 (green), CD68 (red), EdU (white). Bar 50µm (left: Ccl2$^{MC+/+}$; right: Ccl2$^{MC\Delta/\Delta}$). (**h**) Gating strategy for CD45$^{+}$ CD64$^{high}$ MERTK$^{high}$ CD11c$^{low}$ interstitial MΦs in Ccl2$^{MC\Delta/\Delta}$ and Ccl2$^{MC+/+}$ mice. (**i**) Quantification of interstitial MΦs and alveolar MΦs among all CD45$^{+}$ leukocytes (n=5-6 mice/group). (**d**), (**i**) Two-tailed Student's t-test was used. (**f**) Mixed-effects model was used. *P < 0.05. Bar graphs show mean with s.e.m.

# Supplementary Figure 2

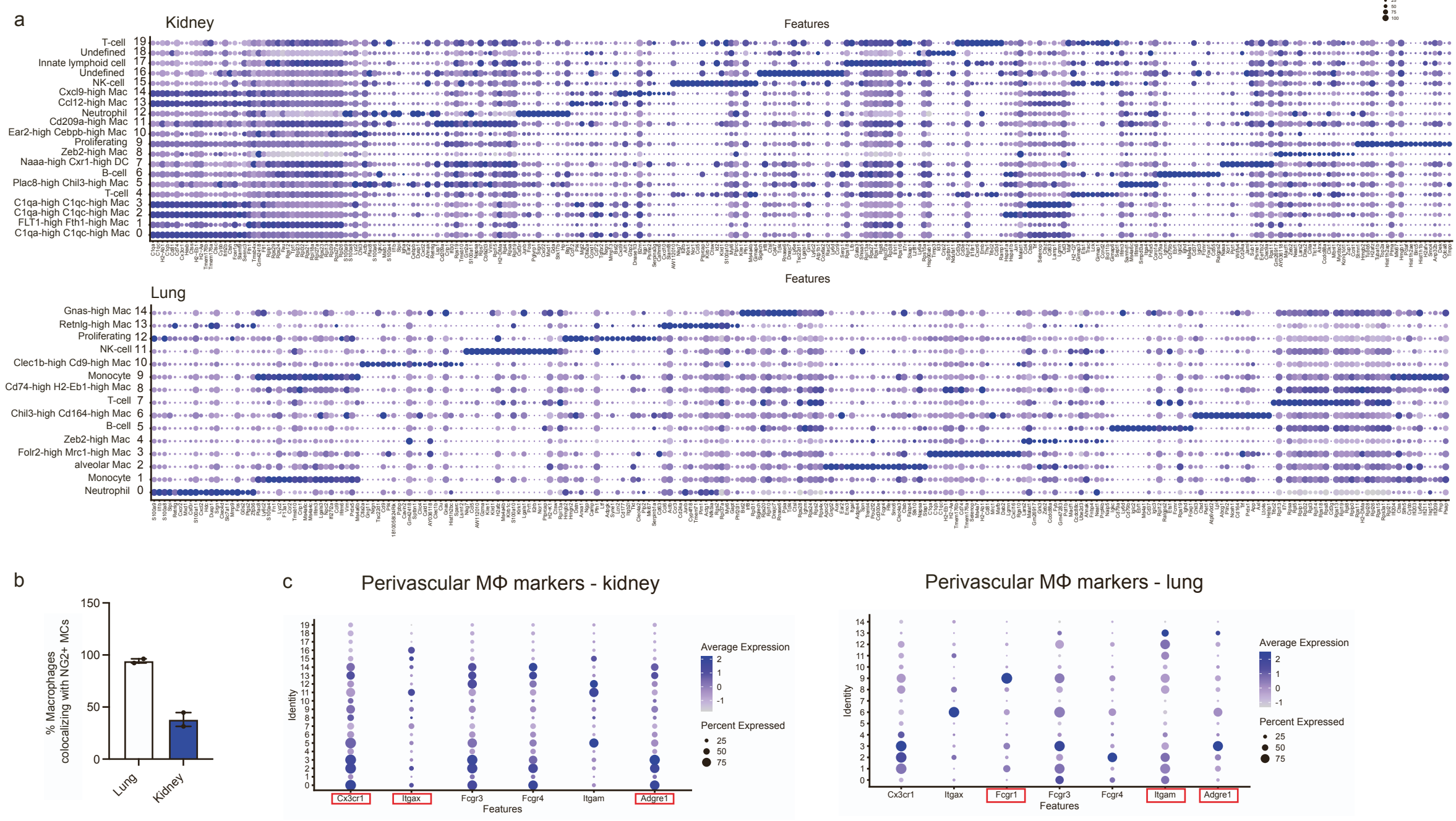


b




c

Perivascular MΦ markers - kidney




Perivascular MΦ markers - lung




d

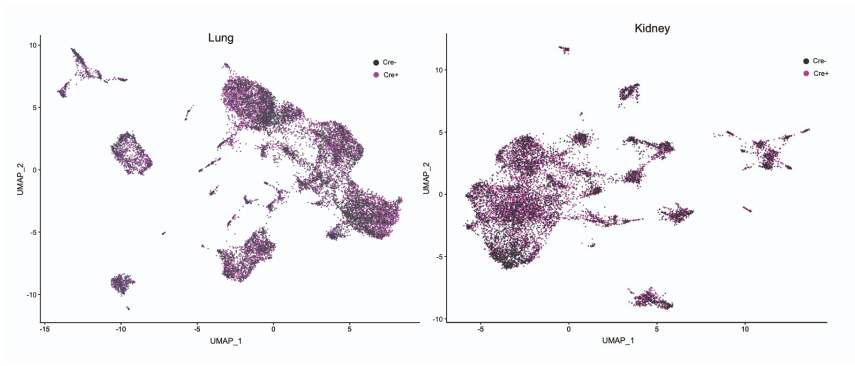


e

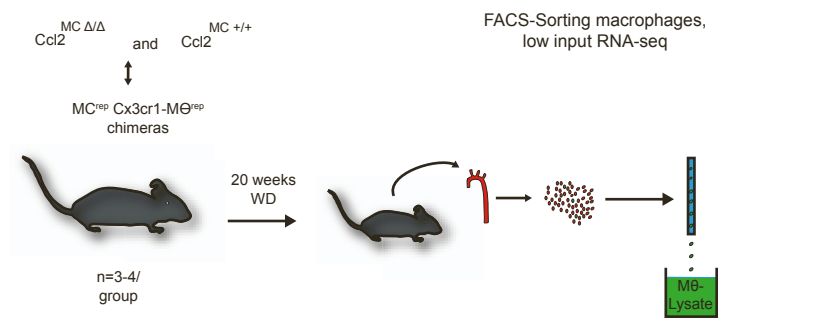


f

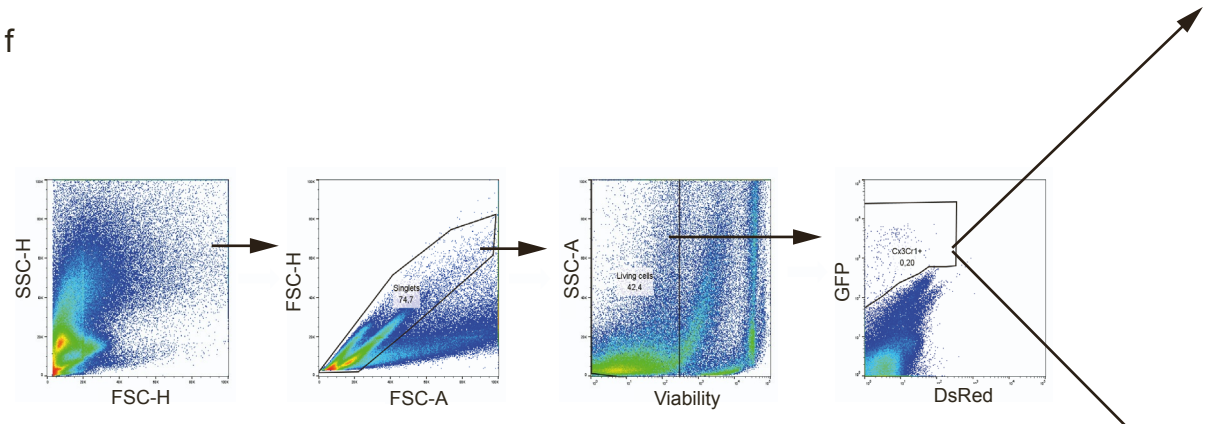


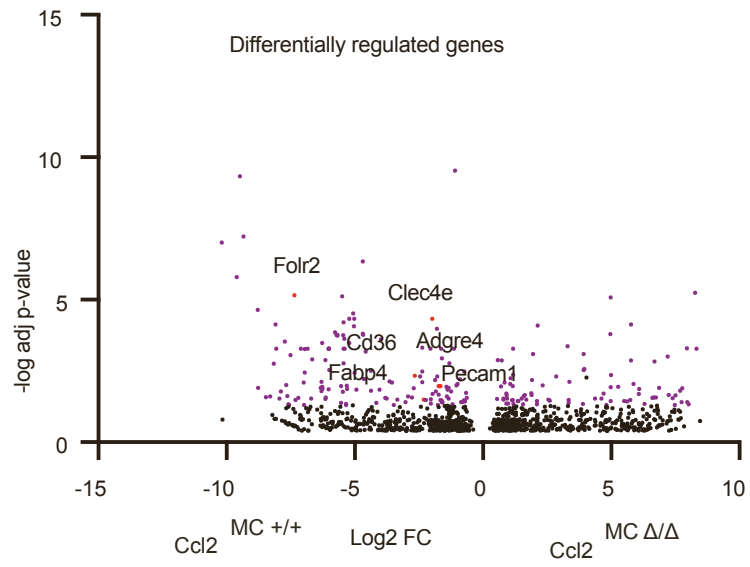


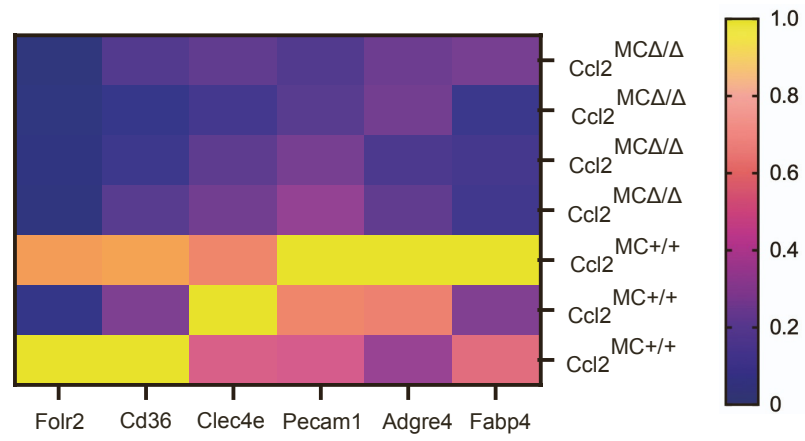


g

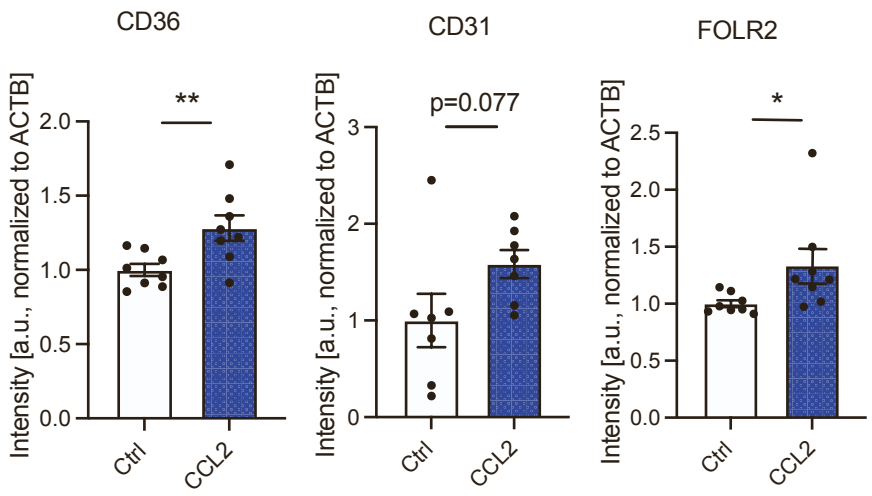


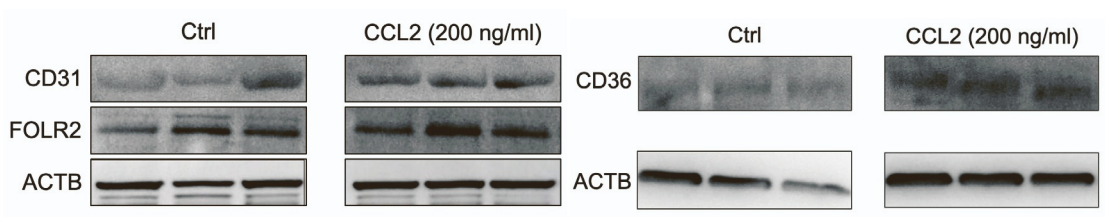

Suppl. Fig. 2 - Phenotypic changes in vascular MΦs by MC-derived CCL2 (related to Figure 2): (**a**) Dot-plots depicting marker gene expressions of all clusters in lung and kidney from single-cell RNA Seq experiments further analyzed in Fig. 2. (**b**) Analysis of MC contacting MΦs within lung and kidney tissue from 2 $MC^{RFP\text{-}rep}$ Cx3cr1-$MΦ^{GFP\text{-}rep}$ mice. No statistical comparison between both groups was performed. (**c**) Predescribed Marker genes (marked by a red square) of perivascular MΦs within the kidney and lung. (**d**) UMAPs of lung and kidney scRNA-seq data, colour coded by genotype origin from either $Ccl2^{MCΔ/Δ}$ or $Ccl2^{MC+/+}$ mice. (**e**) Schematic illustration of media and intima processing from aortae of $Ccl2^{MC+/+}$ or $Ccl2^{MCΔ/Δ}$ chimera mice with $MC^{RFP\text{-}rep}$ Cx3cr1-$MΦ^{GFP\text{-}rep}$ bone marrow littermates after 20 weeks of Western diet and consecutive FACS-Sorting for macrophages, followed by low input RNA sequencing. (**f**) Left: Gating strategy for FACS sorting of the aorta from $Ccl2^{MC+/+}$ or $Ccl2^{MCΔ/Δ}$ chimera mice with $MC^{RFP\text{-}rep}$ Cx3cr1-$MΦ^{GFP\text{-}rep}$ bone marrow after 20 weeks Western diet. After gating on living singlets *Cx3cr1*$^{GFP}$ cells were sorted into specific lysis buffer. Top right: Volcano plot depicting differentially regulated genes (all genes with a p-value <0.4 included). Significantly regulated genes are colored purple. Genes further depicted in Fig. 2i are colored in red and labelled. Bottom right: Heatmap displaying expression of differentially regulated genes further depicted in Fig. 2i. n=3-4 chimera mice. (**g**) Left: Western blot quantification (Intensitiy, airbitrary units normalized to ACTB) of MΦ lysate for CD36, FOLR2 and CD31 after MΦ stimulation with CCL2. Right: Representative Western Blots. n=8 replicates from a total of n=16 mice. Paired two-tailed t-test was used for normally distributed data. *P < 0.05, **P< 0.01.

Supplementary Figure 3

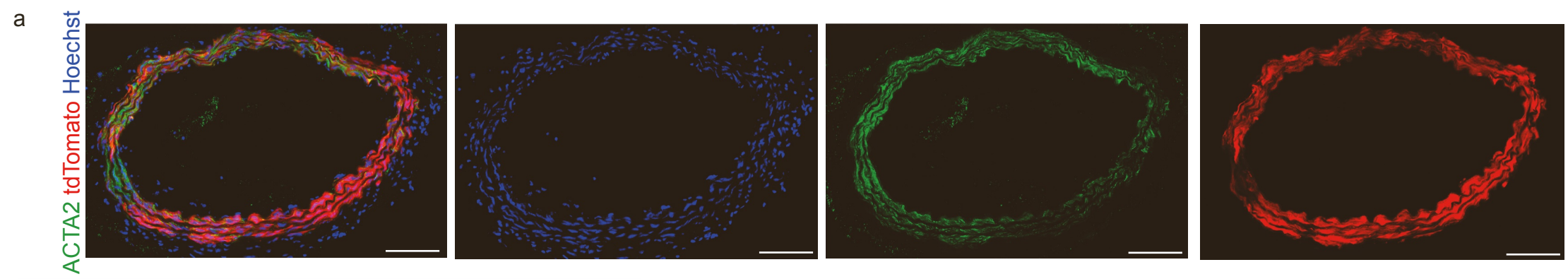


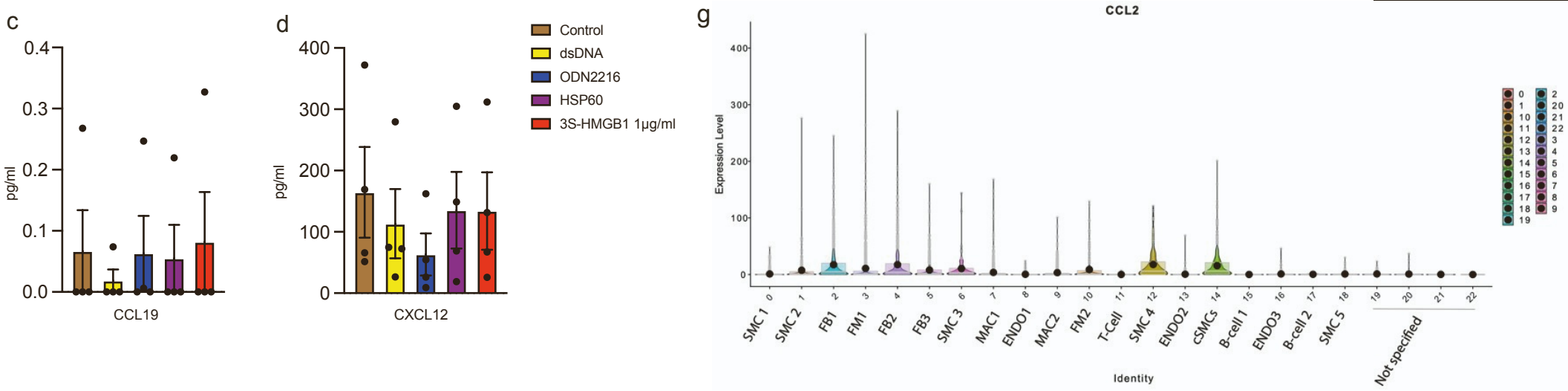


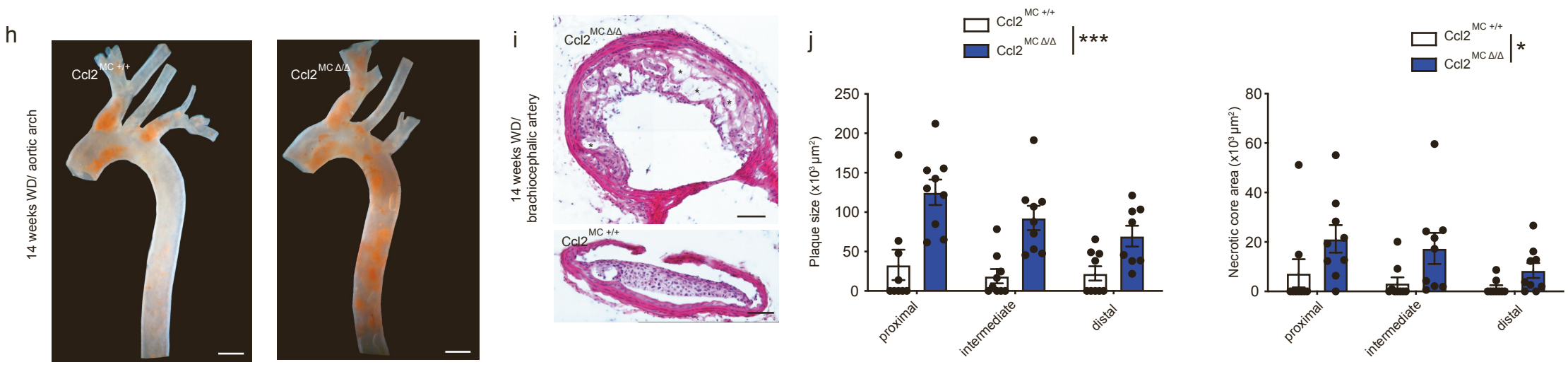


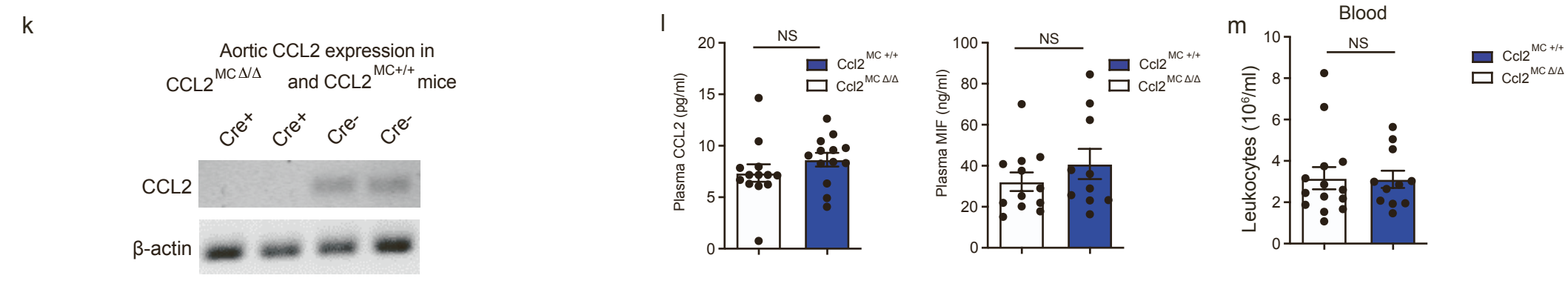


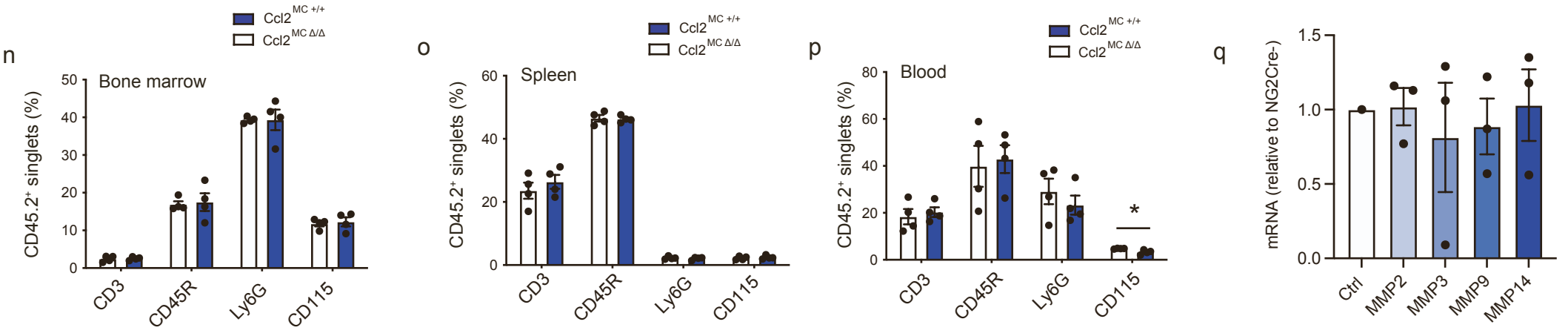

Suppl. Fig. 3 - Mural cells exhibit relevant expression levels of inflammatory chemokines (related to Figure 3): (**a**) Immunofluorescence images of $SMC^{Ca2+\text{-}rep}$ ascending aortas with its endogenous tdTomato signal (red), additionally stained for ACTA2 (α-SMA) (green) and Hochest (blue). Representative of 3 different vascular locations from n=2 mice. Scalebar 100µm. (**b**) Western Blot confirmation of CCL2 and MIF protein levels in HCASMCs at baseline levels and after TNFα stimulation. (**c**) CCL19 protein levels after stimulation of HCASMs with different Toll-like receptor (TLR) agonists. n=4 independent experiments. (**d**) CXCL12 protein levels after stimulation of HCASMs with different TLR agonists. n=4 experiments. (**a**)-(**d**) Mann-Whitney and two-tailed student's t-test were used. (**e**) FACS plots illustrating $DsRed^{+}$ cells in Ng2-DsRed; $ApoE^{-/-}$ ($MC^{RFP\text{-}rep}$) and $ApoE^{-/-}$ aortas. (**f**) FACS-sorted $Ng2^{+}$ SMCs from Ng2-DsRed; $ApoE^{-/-}$ mice. (Scalebar 20µm) (**g**) *Ccl2* expression by different single-cell clusters of a human atherosclerotic lesion. (**h**) En-Face macroscopic Sudan III staining of $Ccl2^{MC\Delta/\Delta}$ and $Ccl2^{MC+/+}$ mice after 14 weeks of Western diet. (Scalebar 1mm). (**i**) Representative H.E. stained BCA sections of $Ccl2^{MC\Delta/\Delta}$ and $Ccl2^{MC+/+}$ mice after 14 weeks of western diet. (Scalebar 100µm). (**j**) Analysis of plaque size and necrotic core area in $Ccl2^{MC\Delta/\Delta}$ and $Ccl2^{MC+/+}$ mice after 14 weeks of western diet. Repeated measures 2-way ANOVA. (**k**) Representative gels from RT-PCR for mRNA encoding CCL2 (top) and β-actin (bottom) of the aorta form $Ccl2^{MC+/+}$ and $Ccl2^{MC\Delta/\Delta}$ mice. (**l**)**,** Plasma levels of CCL2 (left) and MIF (right) in $Ccl2^{MC+/+}$ and $Ccl2^{MC\Delta/\Delta}$ mice after 14 weeks Western Diet (n=10-13 each). **m**-**p,** Quantification of leukocytes in $Ccl2^{MC+/+}$ and $Ccl2^{MC\Delta/\Delta}$ mice after 14 weeks Western Diet: (**m**) Blood leukocyte count (n=11-14 each); Quantification of T cells (CD3), B cells (CD45R), neutrophils (Ly6G) and monocytes (CD115) in bone marrow (**n**), spleen (**o**), and blood (**p**); **n** through **p**, n=4 each. (**q**) RT-PCR analysis of aortic tissue after 12 weeks HFD for MMP2, MMP3, MMP9, and MMP14 mRNA in Cre+ (n=3) relative to Cre- mice (n=3; set as one). (**l**)-(**q**) Two-tailed Student's t-test was used. NS, not significant.***p<0,001, *p<0,05. Bar graphs show mean with s.e.m.

Supplementary Figure 4

## Further characterization of CCL2$^{SMC+/+}$ and CCL2$^{SMC\Delta/\Delta}$ mice

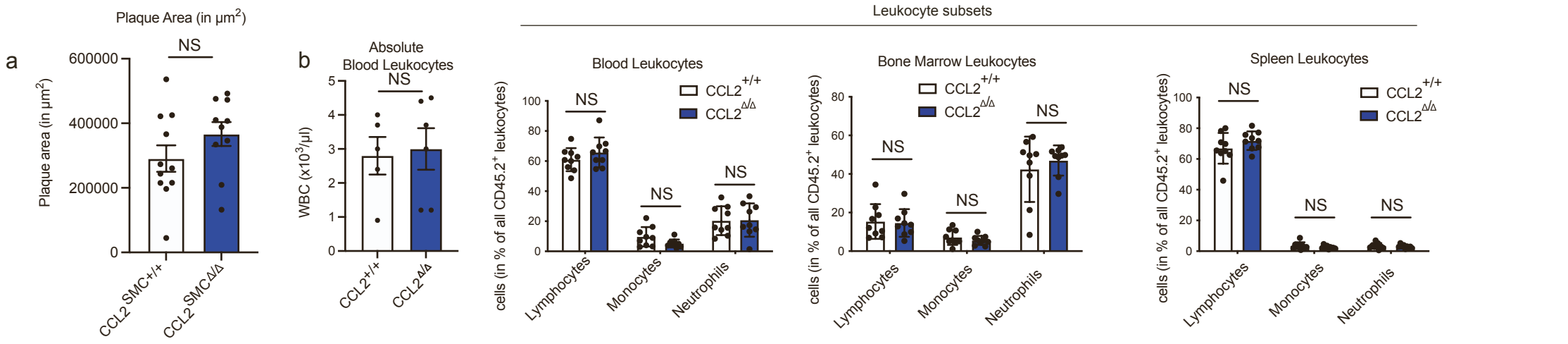


## Knock-out PCR for the CCL2 locus in the vasculature

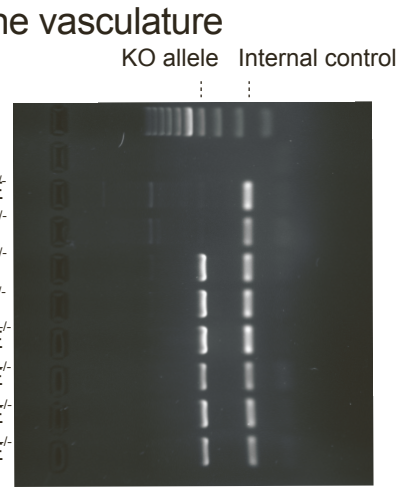


## Characterization of MIF$^{MC+/+}$ and MIF$^{MC\Delta/\Delta}$ mice

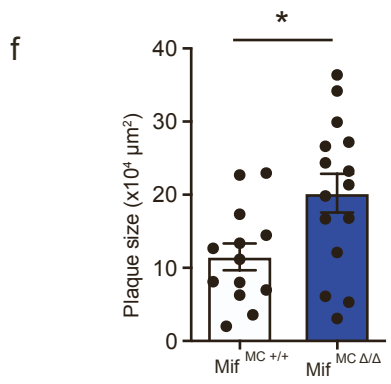


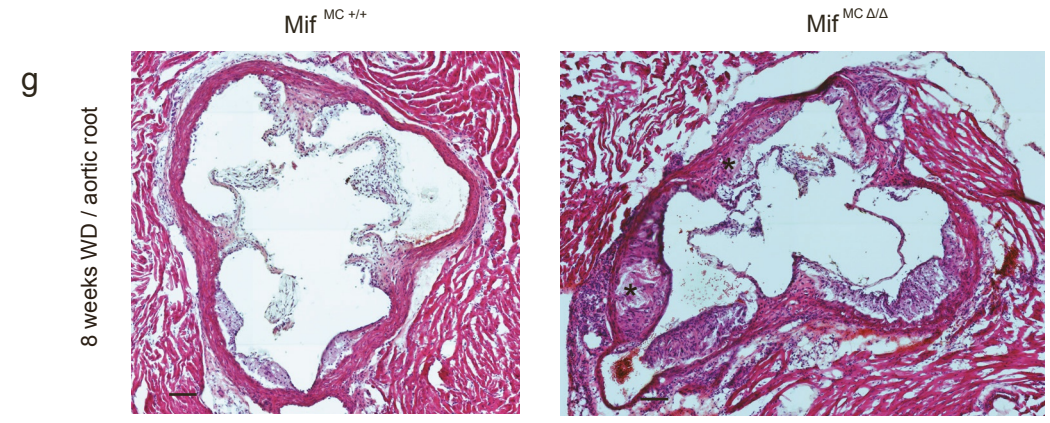


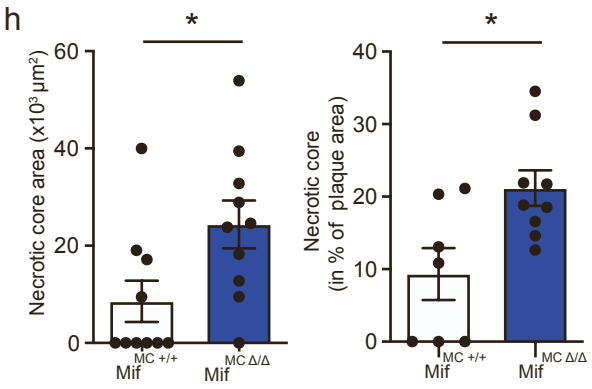


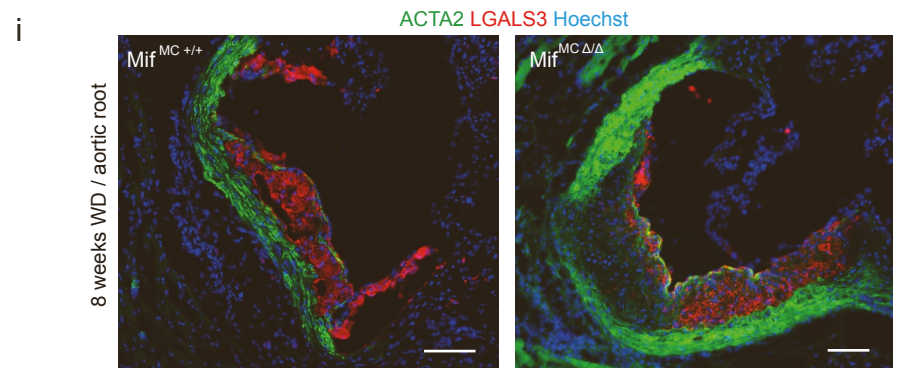


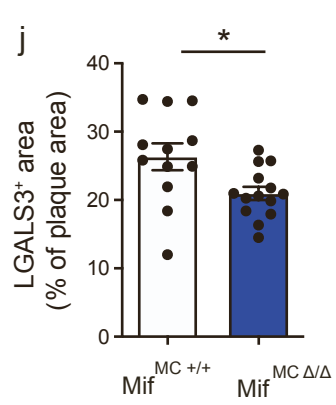


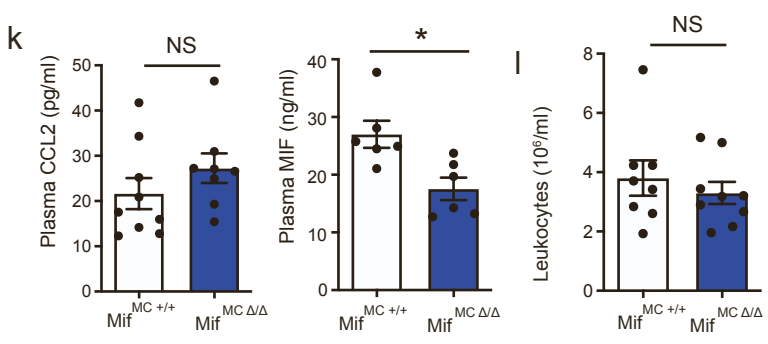


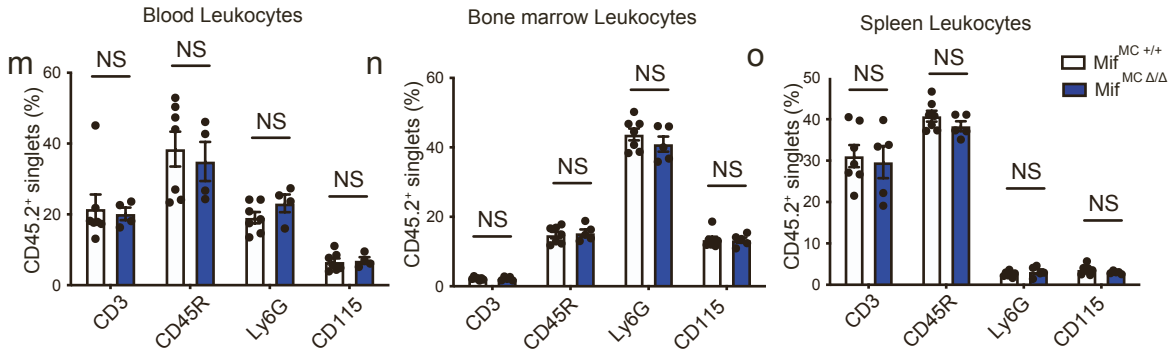


p

| | NG2Cre⁻MIF$^{fl/fl}$ ApoE$^{-/-}$ | NG2Cre⁺MIF$^{fl/fl}$ ApoE$^{-/-}$ | significance |
|---|---|---|---|
| Weight (g) | 31.625 ± 6.06 | 31.4± 1.14 | NS |
| Cholesterol (mg/dl) | 843.8 ± 321.1 | 643.2 ± 208.8 | NS |

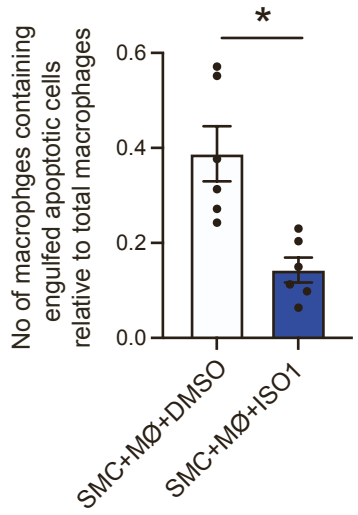


## Knock-out PCR for the MIF locus in the vasculature

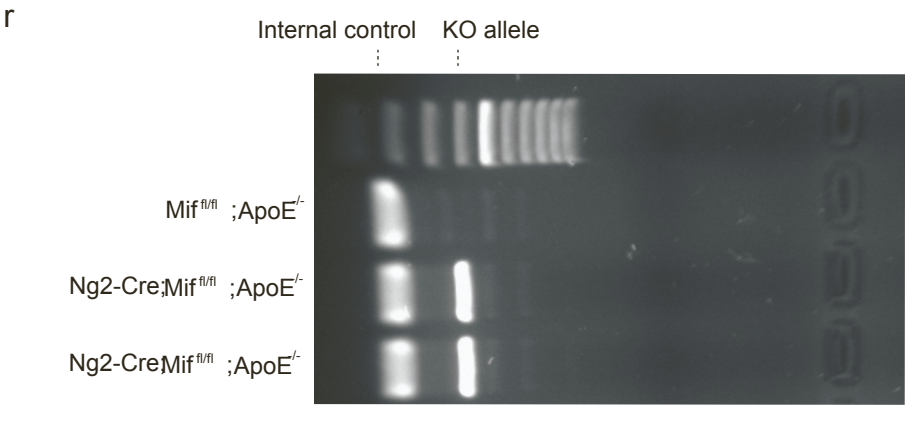

Suppl. Fig. 4 - MΦ active chemokines derived from mural cells are atheroprotective (related to Figure 3): (**a**) Morphometric analysis of plaque size from valvular sections from $Ccl2^{SMC+/+}$ and $Ccl2^{SMC\Delta/\Delta}$ littermates (n=10-11). (**b**) Absolute leukocyte counts (n=5-6), leukocyte subset distribution in blood (left), bone marrow (middle) and spleen (right) from $Ccl2^{SMC+/+}$ and $Ccl2^{SMC\Delta/\Delta}$ littermates (n=9). (**c**), Plasma level of CCL2 in pg/ml (n=5-7), body weight (n=9-11), VLDL/LDL, HDL and total cholesterol in mg/dl (n=8-10) from $Ccl2^{SMC+/+}$ and $Ccl2^{SMC\Delta/\Delta}$ littermates. (**d**) Flow cytometry of atherosclerotic aortas from $Ccl2^{SMC+/+}$ and $Ccl2^{SMC\Delta/\Delta}$ mice analysing mononuclear phagocyte, lymphocyte and neutrophil counts within the aortic tissue (n=3-4 / group). (**e**) PCR for the Knock-Out allele in $Ccl2^{fl/fl;}$ $ApoE^{-/-}$, Myh11-CreERT2; $ApoE^{-/-}$,Myh11-CreERT2; $Ccl2^{fl/fl;}$ $ApoE^{-/-}$ and FACS-Sorted td-tomato$^{+}$ SMCs from Myh11-CreERT2; R26-td-tomato; $Cx3cr1^{GFP}$; $Ccl2^{fl/fl;}$ $ApoE^{-/-}$ mice. (**a**), (**b**), (**c**), (**d**) Two-tailed student's t-test was used. NS, not significant. Data are shown as mean and s.e.m. (**f**) Quantification of plaque size in the aortic valve of $Mif^{MC+/+}$ and $Mif^{MC\Delta/\Delta}$ littermates after 8 weeks Western diet (n=13-15 mice/group). (**g**) Representative images of plaque formation by H.E. staining in the aortic root; * indicates necrotic core. Scalebar 100µm. (**h**)-(**j**), Histologic analysis of the aortic root from $Mif^{MC+/+}$ and $Mif^{MC\Delta/\Delta}$ littermates (n=11-14 each). (**h**) Left: Necrotic core area within the plaque assessed by H.E. staining; Right: Necrotic core area relative to plaque size. (**i**), Representative immunofluorescent images of the aortic valve from $Mif^{MC+/+}$ and $Mif^{MC\Delta/\Delta}$ littermates after 8 weeks Western diet stained for ACTA2 (green), LGALS3 (red), and Hoechst (blue). Scalebar: 100µm. (**j**) Intimal LGALS3$^{+}$ area as percent of plaque size (n=12). (**k**) Plasma levels of CCL2 (left) and MIF (right) (n=6-9 mice/group). (**l**) Blood leukocyte counts (n=8-9 mice). (**m**)–(**o**) Quantification of T cells (CD3), B cells (CD45R), neutrophils (Ly6G) and monocytes (CD115) in blood (**m**), bone marrow (**n**), and spleen (**o**) among CD45$^{+}$ singlets; (**m**)-(**o**), n=4-7 each. (**p**) Body weight, plasma cholesterol from n=5-6 mice as mean and s.e.m. (**q**) *In vitro* efferocytosis assay, analysing the number of macrophages containing engulfed cells relative to all macrophages in the FOV. n=6 from 3 independent experiments. (**r**) PCR for the Knock-Out and Wildtype allele in the macrovasculature of $Mif^{MC+/+}$ and $Mif^{MC\Delta/\Delta}$ mice. (**f**)-(**r**) Lines indicate mean and s.e.m. *P < 0.05. Two-tailed Student's t-test performed for all normally distributed analyses.

# Supplementary Figure 5

Suppl. Fig. 5 - Mural cell derived chemokines induce spatiotemporal MΦ repositioning (related to Figure 4): (**a**) *Ex vivo* 2-photon microscopy of arterial NG2+ cells (red) without (ctrl) or after 14 weeks of Western diet in $MC^{RFP\text{-}rep}$ mice showing morphological changes of SMCs during plaque development in the carotid artery and the descending aorta. Second harmonic generation (SHG) from collagen fibers in blue. Dotted line shows plaque. Scalebar: 20µm. (**b**) Confocal image of an atherosclerotic lesion from a $MC^{RFP\text{-}rep}$ mouse after 6 weeks of Western Diet in the thoracic aorta. Dashed line depicts $NG2^+$ SMCs within the fibrous cap. Scalebar 20 µm. (**c**) Quantification of intimal $NG2^+ACTA2^+$ cells and $NG2^+$ $PDGFR\beta^+$ cells compared to all $NG2^+$ cells in the aortic arch (left) and aortic valve (right) area after 6 and 12 weeks of Western Diet assessed by immunofluorescence staining in $MC^{RFP\text{-}rep}$ mice shown as mean and s.e.m.; n=4 each (Two-tailed student's t-test). ** $P < 0.01$; * $P < 0.05$; # $P = 0.09$ (left). (**d**) Left image: Aortic root epifluorescence imaging of a $MC^{RFP\text{-}rep}$ mouse stained for ACTA2. NG2 in red, ACTA2 in green, Hoechst in blue. Scalebar 50µm. Right image: Aortic arch cross section after 6 weeks Western diet stained for PDGFRβ (green), and Hoechst (blue), $NG2^+$ cells in red. Scalebar 10 µm. (**e**) Flow cytometric visualization of DsRed, GFP expression and overlap single-cells of the aorta from $MC^{RFP\text{-}rep}$ mice after 6 weeks Western Diet (left), $MC^{RFP\text{-}rep}$ Cx3cr1-$M\Phi^{GFP\text{-}rep}$ mice without Western Diet (middle), and $MC^{RFP\text{-}rep}$ Cx3cr1-$M\Phi^{GFP\text{-}rep}$ mice after 12 weeks Western Diet (right). (**f**) Chemotaxis assay with conditioned medium from resting or dsDNA, 3S-HMGB1, disulfide HMGB1, HSP60, or ODN 2216 (with ODN 2243 as control) stimulated HCASMCs compared to medium for human monocytes (n=3 independent experiments). (**g**), (**h**) Inhibition of monocyte chemotaxis by the MIF antagonist ISO-1 (compared to DMSO as vehicle set as 100%) or a CCL2 blocking antibody (compared to isotype antibody set as 100%) in conditioned medium from (**g**) 3S-HMGB1 stimulated HCASMCs incubated with BoxA (n=4 independent experiments) or (**h**) dsDNA stimulated HCASMCs (n=3 independent experiments). (**i**) Chemotaxis assay of monocytes with conditioned medium from dsDNA stimulated HCASMCs in the presence of DNase or control (ctrl) (n=4 independent experiments). NS, not significant. *$P < 0.05$. (**f**)-(**i**) For directional chemotaxis assays one-tailed Student's t-test or Mann Whitney-test was used. (**j**) Violin plots of expression levels of different canonical receptors targeted by CCL2 - CCR2, CCR3, CCR4 & CCR5, across the different single-cell RNA Seq clusters in mouse atherosclerotic lesions, further depicted in Fig. 5a. (**k**) SMC wound healing assay measuring the relative reduction of the original scratch area after 12h and 24h in presence of either an anti-CCL2 antibody, isotype control antibody or without further addition of antibodies (control) (n=3 experiments). (**l**) SMC proliferation assay measuring SMC count / FOV after 0h, 24h and 48h in presence of either an anti-CCL2 antibody, isotype control antibody or without further addition of antibodies (control) (n=3 experiments). (**k**), (**l**), Repeated measures Two-way ANOVA.

Supplementary Figure 6

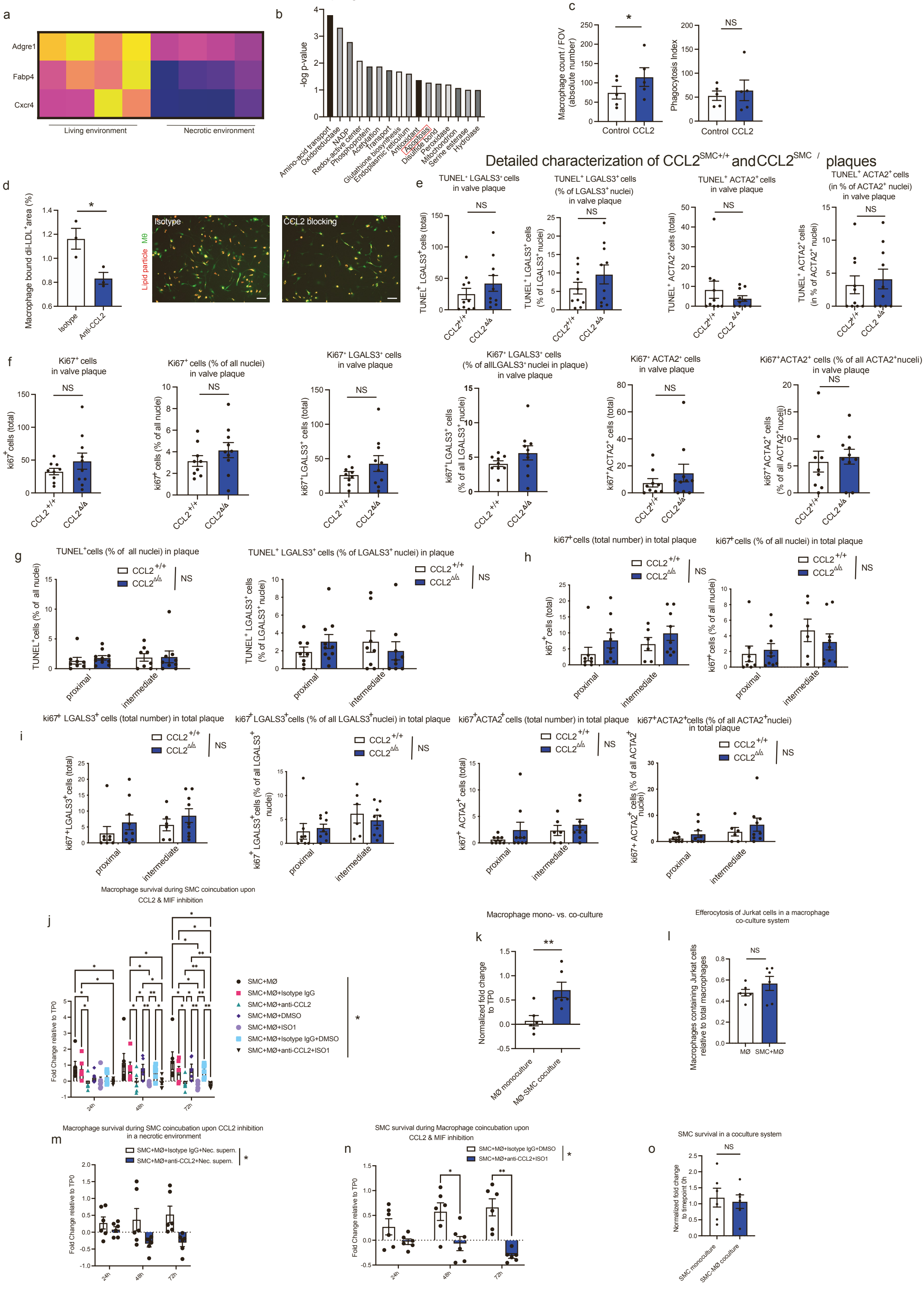

Suppl. Fig. 6 - Survival and function of the MΦ niche are influenced by mural cell derived chemokines (related to Figure 5): (**a**) Heatmap depicting MΦ defining genes analysed in bulk RNA Seq data of FACS-sorted MΦs after coincubation for 12h with either live or necrotic Jurkat cell supernatant. (**b**) Sub-division of UP_KEYWORDS upregulated in MΦs in a necrotic environment, "Apoptosis" pathway is highlighted. (**c**) Quantification of MΦ count per FOV with CCL2 present, compared to medium without CCL2 in peritoneal MΦs from Lyz-MΦ$^{GFP\text{-}rep}$ mice (left), phagocytosis index of MΦs upon presence or absence of CCL2 (right) (n=3 experiments). (**d**) Quantification of macrophage bound dil-LDL$^+$ area upon addition of SMC supernatant with either CCL2-blocking or isotype antibody. Representative epifluorescence images of the cholesterin uptake (red) in peritoneal macrophages from Lyz-MΦ$^{GFP\text{-}rep}$ mice (n=3 experiments). Scalebar 50 µm. (**e**) Quantification of valve atherosclerotic plaques for total and relative TUNEL$^+$ LGALS3$^+$ cells (left), total and relative TUNEL$^+$ ACTA2$^+$ cells (right), n=10 mice/group. (**f**) Quantification of valve atherosclerotic plaques for total and relative KI67$^+$ cells (left), total and relative KI67$^+$ LGALS3$^+$ cells (middle), total and relative KI67$^+$ ACTA2$^+$ cells (right), n=9-10 mice/group. (**g**) Quantification of brachiocephalic artery atherosclerotic plaques at proximal and intermediate sites for relative TUNEL$^+$ cells (left), relative TUNEL$^+$ LGALS3$^+$ cells (middle), relative TUNEL$^+$ ACTA2$^+$ cells (right), n=9-10 mice in total/group. (**h**) Quantification of brachiocephalic artery atherosclerotic plaques at proximal and intermediate sites for total and relative KI67$^+$ cells, (**i**) Quantification of brachiocephalic artery atherosclerotic plaques at proximal and intermediate sites for total and relative KI67$^+$ LGALS3$^+$ cells (middle), total and relative KI67$^+$ ACTA2$^+$ cells (right), (**h**), (**i**) n=8-9 mice/group. (**c**), (**d**), (**f**) Two-tailed Student's t-test was used. (**e**), Two-tailed Student's t-test was used for graphs on the left, Mann-Whitney test was used for the graphs on the right examining ACTA2$^+$ cells. (**g**), (**h**), (**i**) Mixed-effects model. *P < 0.05. Bar graphs show mean with s.e.m. (**j**) Coincubation of SMCs and MΦs, coincubation of SMCs and MΦs with addition of isotype IgG (red), coincubation of SMCs and MΦs with addition of anti-CCL2 antibody (purple), coincubation of SMCs and MΦs with addition of DMSO (white) as vehicle control for the MIF antagonist ISO1, coincubation of SMCs and MΦs with addition of MIF antagonist: ISO1 (orange), coincubation of SMCs and MΦs with addition of Isotype IgG and DMSO (brown), coincubation of SMCs and MΦs and addition of anti-CCL2 antibody and MIF antagonist: ISO1. Analysis of MΦ counts. (**k**) Analysis of MΦ survival in SMC-MΦ coculturing system compared to MΦs in monoculture relative to total macrophage count at timepoint 0 (TP0). (**l**) Analysis of MΦs containing apoptotic Jurkat cells, relative to total macrophage count in either a macrophage mono- or SMC-macrophage coculturing system. (**m**) Analysis of MΦ counts in a SMC-MΦ coincubation system in a necrotic environment of dead Jurkat cell supernatant either with Isotype IgG or with anti-CCL2 antibody. (**n**) Coincubation of SMCs and MΦs with addition of Isotype IgG and DMSO (as a vehicle control of the MIF antagonist ISO1) compared to coincubation of SMCs and MΦs and addition of anti-CCL2 antibody and MIF antagonist: ISO1. Analysis of SMC counts relative to timepoint 0 (TP0). (**o**) Analysis of SMC survival in SMC-MΦ a coculturing system compared to SMCs in monoculture relative to total macrophage count at timepoint 0 (TP0). (**j**), (**m**), (**n**) Repeated measures two-way ANOVA or mixed-effects model with subsequent Fisher's LSD Test was used. (**k**), (**l**), (**o**) Two-tailed Student's t-test was used. (**j**)-(**o**) n=6 replicates from 3 independent experiments. *P < 0.05; NS, not significant. Bar graphs show mean with s.e.m.

| Strain name | Given name | Function |
|---|---|---|
| *Cx3cr1$^{Cre-ERT2}$; PC-G5-tdT* | Cx3cr1-MΦ$^{Ca-rep}$ | *In vivo* visualization of calcium activity in and spatiotemporal distribution of MΦs |
| *Cx3cr1$^{GFP}$* | Cx3cr1-MΦ$^{GFP-rep}$ | *In vivo* and *ex vivo* labelling of mononuclear phagocytes across the vasculature |
| *Ng2-DsRed; ApoE$^{-/-}$* | MC$^{RFP-rep}$ | *In vivo* and *ex vivo* labelling of mural cells in the microvasculature as well as the homeostatic or inflammed macrovasculature |
| *Ng2$^{DsRed}$; Cx3cr1$^{GFP}$; ApoE$^{-/-}$* | MC$^{RFP-rep}$ Cx3cr1-MΦ$^{GFP-rep}$ | Labelling arterial and arteriolar pericytes as well as smooth muscle cells and simultaneously Cx3cr1$^{+}$ MΦs |
| *Ng2$^{DsRed}$; Lyz2$^{eGFP}$; ApoE$^{-/-}$* | MC$^{RFP-rep}$ Lyz-MΦ$^{GFP-rep}$ | Labelling arterial and arteriolar pericytes as well as smooth muscle cells and simultaneously Lyz2$^{+}$ MΦs |
| *Ng2$^{cre}$; Ccl2$^{fl/fl}$; ApoE$^{-/-}$* | Ccl2$^{MCΔ/Δ}$ | Investigation of the effects of CCL2 derived from MCs on MΦ phenotype |
| *Myh11$^{cre-ERT2}$; PC-G5-tdT* | SMC$^{Ca2+-rep}$ | Investigation of SMC calcium signaling upon incubation with necrotic cell supernatant or control |
| *Ng2-cre; Mif$^{fl/fl}$; ApoE$^{-/-}$* | Mif$^{MCΔ/Δ}$ | Investigation of the effects of MIF derived from MCs on MΦ phenotype |
| *Myh11$^{cre-ERT2}$; Ccl2$^{fl/fl}$; ApoE$^{-/-}$* | Ccl2$^{SMCΔ/Δ}$ | Investigation of the effects of CCL2 derived from SMCs on MΦ phenotype |
| *Myh11$^{cre-ERT2}$; Rosa26$^{tdT}$; Cx3cr1$^{GFP}$; ApoE$^{-/}$* | SMC-tdT$^{lin}$ Cx3cr1-MΦ$^{GFP-rep}$ | Fate-mapping pericytes as well as smooth muscle cells during atheroprogression and simultaneously Cx3cr1$^{+}$ MΦs |
| *Myh11$^{cre-ERT2}$; Rosa26$^{tdT}$; Cx3cr1$^{GFP}$; Ccl2$^{fl/fl}$; ApoE$^{-/-}$* | Ccl2$^{SMCΔ/Δ}$ SMC-tdT$^{lin}$ Cx3cr1-MΦ$^{GFP-rep}$ | Investigation of the effects of CCL2 derived from SMCs on MΦ phenotype with simultaneous fate-mapping of SMCs during atheroprogression |
| *ApoE$^{-/-}$* | ApoE$^{-/-}$ | For CCL2 inhibition experiments, these mice were employed for allowing atherosclerotic disease induction |

**Suppl. Table 1:** Strain name, given name and function of all genetic deletion strain combinations employed in the manuscript.